THE PENNSYLVANIA STATE UNIVERSITY
SCHREYER HONORS COLLEGE

DEPARTMENT OF BIOCHEMISTRY AND MOLECULAR BIOLOGY

DETERMINING BRAIN REGIONS UNDERLYING AN ANTIDEPRESSANT-LIKE PHENOTYPE IN MICE

CHRISTIAN JAMES MORRIS
SPRING 2018

A thesis
submitted in partial fulfillment
of the requirements
for a baccalaureate degree
in Biochemistry and Molecular Biology
with honors in Biochemistry and Molecular Biology

Reviewed and approved* by the following:

Bernhard Lüscher
Professor of Biology and Biochemistry & Molecular Biology
Thesis Supervisor

Ming Tien
Professor of Biochemistry & Molecular Biology
Honors Adviser

* Signatures are on file in the Schreyer Honors College.

ABSTRACT

Major Depressive Disorder (MDD) is a highly phenotypically diverse and disabling psychiatric disorder that affects up to 17% of the U.S. population at least once in their lives (Kessler et al., 2003). Studies of human patients and animal models suggest that imbalances between neurotransmission by the main inhibitory and excitatory neurotransmitters, GABA and glutamate, respectively play a key role in MDD. Somatostatin-positive (SST^+) neurons are one of the three major subtypes of GABAergic inhibitory neurons of the brain. A recent study in our lab investigated the emotion-related behavior of SSTCre:$\gamma2^{f/f}$ mice with $\gamma2^{f/f}$ control mice. These mice feature a conditional γ2 subunit deletion in only SST cells. SST GABAergic interneurons have been implicated in mood disorders, making them a cell population of interest. The γ2 subunit plays a critical role in postsynaptic accumulation of $GABA_A$Rs, and deletion of this subunit directly causes functionally impaired GABAergic inhibition. Electrophysiological analyses of SST^+ cells of layers 2 and 3 of the anterior cingulate cortex and CA1 of the ventral hippocampus have shown these cells to be constitutively hyperexcitable when compared to $\gamma2^{f/+}$ controls.

The aim of this experiment was to establish an immunohistochemical technique that allows monitoring of the activity of neurons globally while also elucidating which brain regions and cell populations show increased SST^+ cell activity.

I investigated the activity of SST^+ cells of the medial prefrontal cortex (mPFC) and CA1 stratum oriens (S. oriens) using immunofluorescent staining for the c-Fos protein, which is established to reliably detect stress-induced neuronal activity in rodents. After inducing the expression of c-Fos through an acute stressor, the mice are perfused with fixative, their brains

sectioned and stained and subjected to confocal imaging, and then the images of these sections quantified. I found that in S. oriens of SSTCre:$\gamma 2^{f/f}$ mice there was a strong statistical trend indicating an increased percentage of Fos-expressing SST^+ cells in this region following an acute stressor. This finding indicates the successful optimization of a protocol for identifying SST^+ cells that are activated following a stressor and can be applied to other brain regions and SST^+ cell populations of interest.

.

TABLE OF CONTENTS

LIST OF FIGURES

ACKNOWLEDGEMENTS

I would like to thank Dr. Bernhard Luscher for allowing me to join his lab and participate in his research. His advice and support have been crucial during the planning and troubleshooting of experiments conducted for my thesis. I would like to thank those who have worked alongside me in the Luscher lab, Sarah Jefferson, Mengyang Feng, Nikki Crowley, and Yao Guo, for their help in teaching me techniques and helping me whenever I needed it. The guidance and aid provided by all those in the Luscher lab have helped me grow as a premedical student and scientist.

I would also like to thank my family and friends for their encouragement and support. Their collective support has been invaluable, and it seems an understatement to say that I would have not been able to do this without them.

Lastly I would like to thank the The Pennsylvania State University for their generous financial support during my research experience.

Chapter 1

Introduction

GABAergic Deficit Hypothesis of MDD

Deficits in GABAergic transmission have been correlated with MDD in humans and are causative for depressive-like phenotypes in rodent models. Humans diagnosed with MDD were observed to have alterations to their $GABA_AR$ subunit composition as well as lowered GABA concentrations in cerebrospinal fluid (CSF) (Sanacora et al., 1999; Sanacora et al., 2004; Sanacora et al., 2006). Evidence has implicated GABAergic transmission as critical for ventral hippocampus response to stress in addition to modulating the HPA-axis mediated stress response (Cullinan et al. 1993; Maggio & Segal 2009). This implicates GABAergic transmission deficits as a causative agent in anxiety disorders, which have been found to have large comorbidity with mood disorders (Kauffman & Charney 2000). Other investigations were able to identify deficits in GABAergic transmission as a possible causative agent in MDD (Luscher et al., 2011). However, evidence that GABAergic transmission deficits exist in anxiety as well as personality disorders suggest a more complex and integrated role of GABAergic transmission (Reynolds et al., 2004). In contrast, $GABA_AR$ gene expression alteration in depressed and non-depressed suicide victims indicates that these alterations are depression specific (Sequeira et al. 2009; Merali et al., 2004). These studies have implicated GABAergic transmission alterations in mood disorders, but it was not until studies of mice lacking the γ2 subunit of the $GABA_AR$ that GABAergic transmission deficits became known as causal to mood disorders (Luscher et al., 2011).

Our lab created a transgenic mouse model with haploinsufficiency of the γ2 ($\gamma2^{+/-}$) subunit of $GABA_A$Rs that exhibits partly drug resistant depressive-like symptoms and cognitive deficits that are reminiscent of treatment MDD. The γ2 subunit was deleted, because its association with the postsynaptic scaffold protein gephyrin has been found to be necessary and sufficient for $GABA_A$R localization to the postsynaptic membrane sites (Essrich et al., 1998; Schweizer et al., 2003). In addition, γ2-containing $GABA_A$Rs make up 90% of all $GABA_A$Rs, making it the most abundant $GABA_A$R subunit in all of the CNS (Gunther et al., 1995) Without the ability to reach the postsynaptic membrane, γ2-deficient $GABA_A$Rs are inherently useless, resulting in modest but significant defects in inhibitory synaptic transmission even when only one allele of this gene is deleted (Crestani et a 1999; Ren et al 2016). We found that this effect lead to an inability to maintain a healthy excitation:inhibition (E:I) balance and resulted in a behavioral model of depressive disorders in mice. The necessity for a normal synaptic E:I balance is supported by the finding that lowered glutamate levels accompany lowered GABA levels in MDD patients (Niciu et al. 2014), suggesting that there are homeostatic self-tuning mechanisms that compensate for defects in inhibitory transmission and help maintain synaptic E:I balance.

Mice heterozygous for γ2 subunit were found to have reduced benzodiazepine binding sites and anxiogenic- and depressive-like phenotypes, correlating molecular deficits with behavioral deficits (Crestani et al., 1999; Earnheart et al., 2007; Shen et al., 2010). In the forced swim test (FST), $\gamma2^{+/-}$ mice became immobile faster and spent more total time immobile than wild type controls, and in the novelty-suppressed feeding test (NSFT), $\gamma2^{+/-}$ mice had an increased latency to feed following food deprivation than did wild type controls (Fuchs & Jefferson et al., 2017). Furthermore, treatment of $\gamma2^{+/-}$ mice with the tricyclic and selective

serotonin reuptake inhibitor (SSRI) antidepressants desipramine and fluoxetine was able to reverse these behaviors to those of wild type controls (Fuchs & Jefferson et al., 2017). In a separate experiment, it was found that cells with homozygous $\gamma 2^{-/-}$ deletion had lower frequency and amplitude of IPSCs compared to wild type controls, confirming that this mutation directly causes lowered levels of inhibitory transmission in cells with the deletion (Fuchs & Jefferson et al., 2017). Taken together, these findings illustrate a causal link between deficits in inhibitory transmission and anxiogenic- and depressive-like brain states in mice.

Somatostatin-positive Interneurons and Depression

Somatostatin-positive (SST^+) cells constitute 20-25% of all interneurons in the cortex and they are known to mainly target the distal dendrites of pyramidal cells, thereby gating the excitatory input from glutamatergic afferent to these cells (Gonchar et al., 2007; Violett et al., 2008). SST^+ GABAergic interneurons provide feed-forward inhibition in the hippocampus and neocortex, and their enhanced function has been shown to mimic the effect of anxiolytic and antidepressant drugs (Engin et al., 2008; Wang et al., 1987). An important population of SST^+ interneurons resides in the S. oriens of the hippocampus and targets parvalbumin interneurons and the apical dendrites of pyramidal cells in the S. lacunosum moleculare (Pfeffer et al., 2013). These interneurons gate glutamatergic input from the entorhinal complex to pyramidal cells, so the activity of these cells is uniquely sensitive to alterations to their reception of GABAergic signals (Leao et al., 2012). Their gating behavior also results in the scaling of their activity with that of their network, most notably in the modulation of the theta frequency, which is a characteristic shown to be enhanced by anxiolytic and antidepressant drugs (Buzsaki at al., 2000; Fanselow et al., 2008). These findings suggest that SST^+ interneuron activity would be

implicated in mood disorders. Indeed, the expression of the SST protein in postmortem brains of human patients has been found to be reduced, a phenomenon replicated in stress-based mouse models of MDD (Tripp et al. 2011; Lin & Sibelle 2013).

Our lab investigated the association between SST^+ neurons and psychiatric disorders in a series of molecular and behavioral assays that verified that increased SST^+ neuron activity yields the molecular and behavioral end points elicited by anxiolytic drugs (Fuchs and Jefferson et al., 2017). A transgenic mouse line was developed that featured a selective deletion of both copies of the gene for the γ2 subunit of $GABA_A$Rs in SST^+ cells through a Cre-lox system. This system allows selective deletion of genes in a specific population of cells via copying the promoter for a gene uniquely expressed in the population and inserting the Cre recombinase gene immediately downstream of this promoter. Cre recombinase is a viral protein that normally performs recombination of viral genes into the host genome by taking two forward facing loxP sequences and inverting the downstream site so that the former 3' end of the downstream loxP site is juxtaposed to the 3' end of the upstream loxP site. When a gene is placed between two forward facing loxP sites, the gene is effectively deleted from the genome.

Our lab's model features a γ2 gene flanked by loxP sites, or "floxed", and the SST promoter-controlled Cre gene is inserted into the genome. The result is a mouse with all SST^+ cells having deleted both copies γ2 gene and all other cells having repressed Cre expression and the loxP sites flanking the gene of interest remaining null as Cre is not present. The mice with these characteristics were coined SSTCre:$\gamma2^{f/f}$ mice for their selective SST^+ cell Cre expression and the floxing of both copies (f/f) of the γ2 gene. Because of the deletion of the γ2 subunit, $GABA_A$Rs are unable to localize to synaptic membranes, and GABAergic transmission to these cells will effectively fall on deaf ears.

The SSTCre:$\gamma2^{f/f}$ mouse was designed to test the hypothesis that increasing GABAergic transmission would elicit an antidepressant-like phenotype when compared to $\gamma2^{+/-}$ controls. $\gamma2^{+/-}$ mice are heterozygous for a deletion of the γ2 subunit; homozygous mice do not survive past post-natal week 2 (Earnheart et al., 2007). This genotype is not dependent on the Cre-lox system. In $\gamma2^{+/-}$ mice, all neurons have the deletion, so inhibitory transmission is globally handicapped. As the mice with the heterozygous deletion exhibited depressive-like phenotypes, it was hypothesized that creating mice with the heightened GABAergic transmission should produce an antidepressant-like phenotype. Because SST^{+} interneurons are so crucial to maintenance of network activity in cell populations that are specifically vulnerable to stress in addition to having concentration deficits in MDD patients (Tripp et al., 2011), they were chosen as the interneuron subtype to make hyperexcitable. Our lab first confirmed the molecular function of the SSTCre:$\gamma2^{f/f}$ mice and subsequently examined the behavioral phenotypes of these mice.

SSTCre:$\gamma2^{f/f}$ mice were observed to have hyper excitable SST^{+} cells that corroborated the molecular design of the experiment, and behavioral assays of these mice showed anxiolytic phenotypes. SSTCre:$\gamma2^{f/f}$ mice, or mutants, were compared to SSTCre:$\gamma2^{f/+}$ heterozygous mice, or controls, which only had one copy of the γ2 gene floxed and another without loxP sites. Mutant mice were found to have significantly lower sIPSC and mIPSC frequencies and amplitudes than controls. Moreover, application of bicuculline, a $GABA_AR$ antagonist, caused input resistance of control mice to be increased to the levels seen in mutant mice, demonstrating that the SSTCre:$\gamma2^{f/f}$ genotype produces SST^{+} cells with inhibitory synaptic inputs equal to cells who have $GABA_ARs$ pharmacologically blocked. Importantly, heightened sIPSC frequency in principal cells complemented the heightened excitability of their presynaptic SST^{+} cells when compared to SSTCre:$\gamma2^{f/+}$, $\gamma2^{f/+}$, and $\gamma2^{+/+}$ controls. This provided the proof-of-concept finding

that heightened SST^+ interneuron activity results in increased inhibitory transmission to the cells on which their axons synapse. Biochemical changes in SSTCre:$\gamma2^{f/f}$ mice were consistent with those found in rodents treated with antidepressant drugs. Specifically, we observed reduced phosphorylation of T56 of eEF2. This phenomenon is consistent with increased translation elongation of eEF2-target mRNAs which was observed in mice treated with 5-HT2C antagonists or ketamine (Opal et al., 2014; Autry et al., 2011; Ren et al., 2016).

Results of behavioral tests sensitive to anxiolytic and antidepressant drug treatment indicated anxiolytic- and antidepressant-like phenotypes in SSTCre:$\gamma2^{f/f}$ mice compared to controls. SSTCre:$\gamma2^{f/f}$ mice were observed to have a higher percentage of open arm entries and percentage of total time on open arms in the elevated plus maze (EPM), and female SSTCre:$\gamma2^{f/f}$ mice had a significantly lower latency to feed in the novelty suppressed feeding test (NSFT), consistent with an anxiolytic phenotype. Assays for antidepressant-like phenotypes included the forced swim test (FST) and learned helplessness test (LHT). In the FST, SSTCre:$\gamma2^{f/f}$ mice had higher latency to first immobility and lower total time immobile, and in the LHT male mice showed a lower number of escape failures. The results from these two assays indicate significantly lowered anhedonic behavior, which is the hallmark of antidepressant drugs.

Thus, behavioral, molecular, and electrophysiological assays all uphold the hypothesis that increased net inhibitory transmission across neural networks is able to produce anxiolytic- and antidepressant-like effects. In my experiment, I further investigate the role of SST^+ cells with a heightened E:I ratio through a novel immunohistochemistry method that is able to mark stress-activated neurons and SST^+ cells and measure their colocalization. This provides insight into the brain regions and circuits in which hyper active SST^+ cells reside and thus insight into the brain regions and circuits in which heightened network inhibitory transmission results in anxiolytic

and/or antidepressant-like effects. Of equal importance is the establishing of a method for identifying neuron-level activity changes that can be applied to future investigations of SST^+ cells and their role in the maintenance of network inhibition following acute stressors.

Fos Expression and Neuronal Activity

Fos is the protein product of the *c-fos* gene, which is a protoconcogene located on human chromosome 14 (citation). Studies of the *c-fos* gene have focused mainly on its protooncogenic properties as well as its use as a marker for neuronal activation (Dragunow et al., 1989; Cruz et al., 2013). The *c-fos* promoter incorporates several elements, including the *cis* inducible element (SIE) serum response element (SRE), and cAMP response element (CRE) (Hayes et al., 1987; Gilman et al., 1986; Sheng et al., 1990). These elements are the targets of signals of diverse sources, including those from IL-2 and IL-6, cAMP, and EGF (Valjent et al., 2003). The use of Fos as a marker for neuronal activation is based on the mechanism of its depolarization and Ca^{2+} influx dependent expression. This activation begins with the NMDA receptor (NMDAR) –mediated Ca^{2+} entry into the cytoplasm following glutamatergic transmission from the presynaptic neuron. Ca^{2+} entry activates calmodulin, which can associate with RasGRF. The calmodulin-RasGRF complex activates Ras, which activates Raf-1, which activates MEK. MEK activates ERK, whose kinase activity is responsible for formation of the transcription preinitiation complex.

The transcription preinitiation complex involves association of the SRE-binding proteins Elk-1 and SRF with CREB via CBP. In order for this association to occur, each needs to be phosphorylated. ERK accomplishes this through direct phosphorylation of Elk-1 and CBP and through activation of the RSK2 kinase (Valjent et al., 2003). RSK2 is responsible for CREB and SRF phosphorylation, which completely primes the complex for association and initiation of transcription. Thus, there is a signaling

cascade directly coupling excitatory synaptic signals to assembly of the transcription preinitiation complex on the CRE- and SRE-containing *c-fos* promoter.

Previous studies have utilized the *c-fos* promoter to couple synaptic activity to a different cellular marker, but the present study will directly use the Fos protein as a means of identifying stress-activated cells. A two-hour period between the forced swim acute stressor and perfusion was chosen as it is the optimal time point for Fos expression following an acute stressor (Viau & Sawchenko, 2002).

Chapter 2

Materials and Methods

2.1 Animals

All animal procedures and experiments were approved by the Pennsylvania State University Institutional Animal Care and Use Committee (IACUC, #46483), and adhered to the guidelines and policies set forth by the National Institutes of Health (NIH).

A total of 12 mice were subjected to the forced swim stressor and sacrificed via perfusion. Mice were of a C57BL/6J (BL6) genetic background. Of the 12 total mice, there were four groups consisting of combination of genotype and sex. Three mice each were female $\gamma2^{f/+}$, male $\gamma2^{f/+}$, female SSTCre:$\gamma2^{f/f}$, and male SSTCre:$\gamma2^{f/f}$. All mice were maintained on a 12-hour light-dark cycle and had *ad libitum* access to food pellets and water.

2.2 Forced Swim Stressor

All 12 mice were subjected to the forced swim stressor for induction of the *fos* gene. The day prior the stressor, mice were singly housed to limit miscellaneous Fos induction the day of the stressor. Mice were placed in a glass beaker filled with 3L of 37^{o}C water for 5 minutes. Following this mice were dried using a paper towel and returned to their cage. After each forced swim stressor all hair and feces were removed. Mice were sacrificed via perfusion 2 hours after the end of the forced swim stressor.

2.3 Perfusion

All 12 mice were sacrificed via cardiovascular perfusion 2 hours after the conclusion of the forced swim stressor. Anaesthetic in the form of 30mL/kg of 1.25% by weight of aqueous 2,2,2-tribromoethanol (avertin) solution. Anaesthetization was confirmed by checking for motor response by squeezing the foot. A medial to lateral incision was made and then extended rostrally until reaching the rib cage. The diaphragm was cut completely from the ventral and lateral portions of the rib cage, and the rib cage was cut from the caudal end of the lateral sides of the rib cage to the rostral limit of the thoracic cavity. The skin flap formed by these incisions was pinned back and a nick made in the right atrium. To the caudal side of the left ventricle a needle was inserted toward the left atrium. Ice-cold phosphate-buffered saline was perfused cardiovascularly for 3 min. followed by 5 min. perfusion with ice-cold 4% PFA. The mouse was perfused with 4% PFA for 5 min. To account for the 30 sec required for fluid to reach the end of the needle from its source, the pump was switched to 4% PFA at 2.5 min. After 4% PFA perfusion, the mouse was decapitated and flesh on the head was peeled back from the incision to reveal the skull. After cutting the occipital bone to allow entry of scissors into the cranial cavity, a cut was made along the rostro-caudal midline of the skull until the nasal bridge was reached. The tips of the scissors were placed into the eye sockets of the mouse and the scissors closed to cut the nasal bridge. The skull was then peeled back using tweezers and the brain removed using a spatula. The perfused brains were post-fixed with 4% PFA for 6 hours at 4^{o}C and then transferred to PBS and stored at 4^{o}C until sectioned.

2.4 Sectioning

Fixed mouse brains were cut into 40 μm sections on a Compresstome VT-300-OZ from Precisionary Intruments. Following transfer from 4% PFA to PBS, mouse brains were cut coronally across the cerebellum to form a flat surface. The brain was then glued onto the Compresstome VT-300-OZ mount on the flat, caudal surface of the brain using one drop of Loctite 404 Instant Adhesive. The metal sleeve was then fitted around the brain and mount and slid back on the mount so that the rostral tip of the olfactory bulb was even with the tip of the sleeve. Melted 4% agarose was poured into the sleeve around the brain until the agarose was level with the end of the sleeve. When agarose was cooled, the mount was inserted into the Compresstome and sectioning was initiated. Sections were collected in groups of 5 sections for sections +1.56 mm from bregma for the mPFC and -3.16 mm from bregma for ventral hippocampus. All sections were stored in PBS containing 0.1% w/v sodium azide until staining to prevent bacterial growth.

2.5 Immunohistochemistry

3 sections from each region for each mouse were stained. First sections were permeabilized in PBS with Triton-100X (1% w/v) on a shaker set to medium agitation for 45 min. at room temperature (25^{o}C). Sections were then blocked in PBS with Triton-100X (0.1% w/v) and normal donkey serum (NDS, 2.5% w/v) for 1 hour at room temperature. Sections were then incubated overnight at 4^{o}C in primary antibody solution containing PBS with 1:500 rabbit α Fos (SYSY, cat. # 226003), 1:500 rat α SST (Millipore, cat. # MaB354), NDS (2.5% w/v), and Triton-100X (0.1% w/v).

Following incubation with primary antibody sections were washed 3x10 min. in PBS with Triton-100X (0.1% w/v). Washed sections were incubated for 1 hour at room temperature in

secondary antibody solution containing PBS with 1:500 Alexa488 α rabbit (raised in donkey), 1:500 Cy3 α rat (raised in donkey), NDS (5% w/v), and Triton-100X (0.1% w/v). Next, sections were washed 3x10 min. at room temperature in PBS with Triton-100X (0.1% w/v). Washed and stained sections were mounted onto VWR frosted microslides (25x75x1mm) using Thermo Fischer Shandon Immumount^{TM} Adhesive and stored at 4^{o}C until imaging.

2.6 Imaging

Sections were imaged on a Zeiss LSM 5 Pascal Confocal Microscope. Images were taken at 200x in the subregions outlined in Figure 1A. Three images were taken for each section. The detector gain and offset were set to 672 and -1.215 for the Fos channel and 745 and -0.157 for the SST channel and adjusted minimally for staining variation between mice. Experimenter was blinded to sex and genotype during imaging. If SST staining was unsuccessful for a mouse, it was discarded. Therefore, sample numbers varied slightly between groups.

2.7 Quantification

Images were quantified using FIJI by ImageJ. Experimenter was blinded to sex and genotype during quantification. Images were loaded onto the software and the split channels action chosen from the image tab on the toolbar. Each red channel (SST) image was thresholded to show only pixels with the top 3% of intensity, and each green channel (Fos) image was thresholded to show only pixels with the top 1% of intensity. For images that did not allow these settings due to overexposure the threshold was set as close to these values as possible. Following this images were stacked by choosing the images to stack action under the images tab stack images option. The analyze particles function was used to detect positive staining with positive

staining requiring groups of 50 pixels. For Fos images whose intensities were not able to be thresholded at the standard percentiles due to being too high, the particle prerequisite of 50 pixels was heightened to 150 pixels to account for the higher number of pixels present in these sections. SST images that did not meet this threshold were quantified manually due to the low number of SST^+ cells per image. Each channel was checked manually to ensure that no chatter marks from sectioning or other non-specific targets were marked as positive signal. Colocalization was determined using the cell counter plugin and manually marking cells that were SST^+ and Fos^+. Averages of Fos^+; SST^+; SST^+, Fos^+; SST^-, Fos^+; and SST^+, Fos^- were calculated for each section (technical replicate). Averages for these counts in each region for each mouse were calculated to find the value for each biological replicate.

2.8 Statistics

All data are presented as the mean +/- S.E.M. All collected data were analyzed and graphed using GraphPad Prism 7 softward (produced by GraphPad Software Inc., La Jolla, California, USA). For comparison of the four genotype and sex groups (female $\gamma2^{f/+}$, male $\gamma2^{f/+}$, female SSTCre:$\gamma2^{f/f}$, and male SSTCre:$\gamma2^{f/f}$) with the Mann-Whitney U test for significance was used. For comparison of the two pooled genotype groups, normality of data was confirmed before using an unpaired two-tailed t test. Differences in data were considered significant if $P<0.05$, and they were interpreted as trends if $P<0.1$.

Chapter 3

Results

Christian Morris genotyped all mice except four $\gamma 2^{f/+}$ mice that were generously provided by Sarah Jefferson. Christian Morris also perfused all mice, post-fixated all brains, sectioned all brains, stained all sections, imaged all sections, quantified all images, statistically analyzed all reported data, and graphed all results.

3.1 Experimental Design

The protocol used in this experiment was based on pre-existing protocol used in our lab for mouse perfusions and immunohistochemistry in brain sections and optimized for Fos expression and SST staining. Immunohistochemical quantification is rooted in the assumption that staining is consistent between all samples. Consistency can be undermined by differing fixation quality, improper duration of post-fixation, inconsistent concentration of antibodies between section groups, and subjective quantification of images. Use of traditional lab protocol for perfusion, post-fixation, and immunohistochemistry yielded poor SST staining that appeared to primarily stain non-specifically in nuclei.

To solve this, several different perfusion flow rates, post-fixation durations, and antibody concentrations were tested for their ability to produce successful SST staining. Perfusion rate of 8 mL/min. was raised to 12 mL/min., and post-fixation time was changed from overnight to 6 hours (Figure 1A). In addition, the immunohistochemistry was attempted using antibodies raised in goat as well as donkey before it was decided that donkey was the better species for our

purposes. Fos expression also needed to be controlled due to the nature of Fos expression to be time dependent (Dragunow et al., 1989). Mice that were stressed and perfused in the same day needed to be staggered so that each mouse had two hours between the end of the stressor to perfusion. Contamination of sections with bacteria was postulated as an issue in initial stainings and was remedied by the addition of 0.1% w/v azide to PBS solutions used to store brains or sections for more than 1 day.

After making these changes, I was able to successfully stain for Fos and SST, which enabled quantification and statistical comparison of their expression. Images were taken in the outlined subregions shown in Figure 1B. For each section three images were taken, and both prefrontal cortex and hippocampal sections were stained in groups of three. This made nine technical replicates for each brain region of each biological replicate. To be quantified, images needed to be thresholded for pixel intensity so that no background staining or overexposed images were included in quantification. This was done by thresholding the Fos channel to show only the top 1% of pixels in terms of intensity were shown and all others were changed to black. The same was done for the SST channel, except this threshold was set to 3%. SST was able to have a higher percent threshold, because SST^+ cells are not as numerous as Fos^+ cells (Figure 3). SST staining is also not as strong as Fos staining, so a lower threshold was necessary.

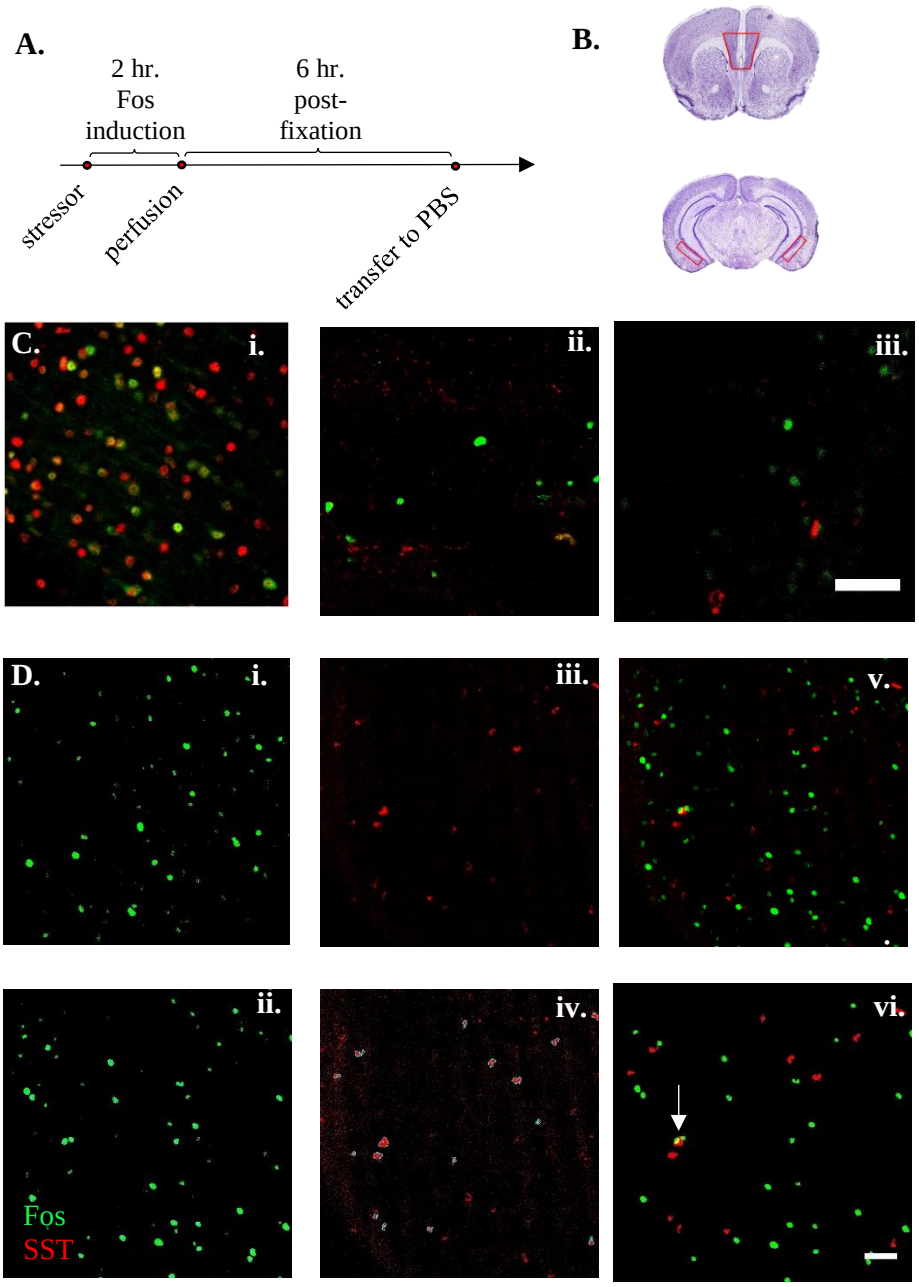

Figure 1: Experimental Design. (A) Diagram of time course of stressor administration, perfusion, and end of post-fixation (transfer to PBS). **(B)** Coronal mouse brain section images from Paxinos Mouse Brain Atlas at +1.54 and -3.16 mm to bregma, respectively, that were used to select sections for staining. Red boxes indicate area of the slice (mPFC and S. oriens of CA1 vHipp, respectively) in which the images were taken. **(C)** Representative 400x images of Fos/SST stainings using different post-fixation durations. (i) 0 hour post-fix. Note nuclear SST staining. (ii) 3 hour post-fix. (iii) 6 hour post-fix. Note cytoplasmic SST staining. Scale bar in Ciii is 50 μm. **(D)** Representative 200x image processing for quantification. (i) Fos staining pre-threshold. (ii) Fos staining post-threshold. All green pixels shown have top 1% intensity value for that image. Particles constituting a cell (>50 pixels) have a light blue outline. (iii) SST staining pre-threshold. (iv) SST staining post-threshold. All red pixels shown have top 3% intensity value for that image. Particles constituting a cell (>50 pixels) have a light blue outline. (v) Merged image pre-threshold. (vi) Merged image post-threshold. Only pixel groups meeting intensity and size requirements (those

outlined in blue in Dii and Div) are shown. Image shows 1 cell with SST^+, Fos^+ colocalization denoted by white arrow. Scale bar in Dvi is 50 μm.

3.2 Representative Images of Immunohistochemistry

The four groups of two different genotypes and both sexes were successfully stained in 19 out of 24 slides or 57 out of 72 sections. The sections from two mice, one male and one female from the mutant groups, had unsuccessful SST staining. One slide containing hippocampal sections of a control male was found to have its brain sections liquefied. During sectioning some of the brains, the Compresstome blade malfunctioned and failed to oscillate momentarily and caused pronounced chatter marks. Chatter marks form elevated rows on sections that occasionally meet intensity and size requirements for being counted as a positive cell. When this occurred, this positive reading was manually omitted. Nonetheless, at least three satisfactory mPFC and hippocampal sections were obtained from each mouse. All sections were stained in one round to prevent differing antibody concentrations between rounds from interfering with staining quality.

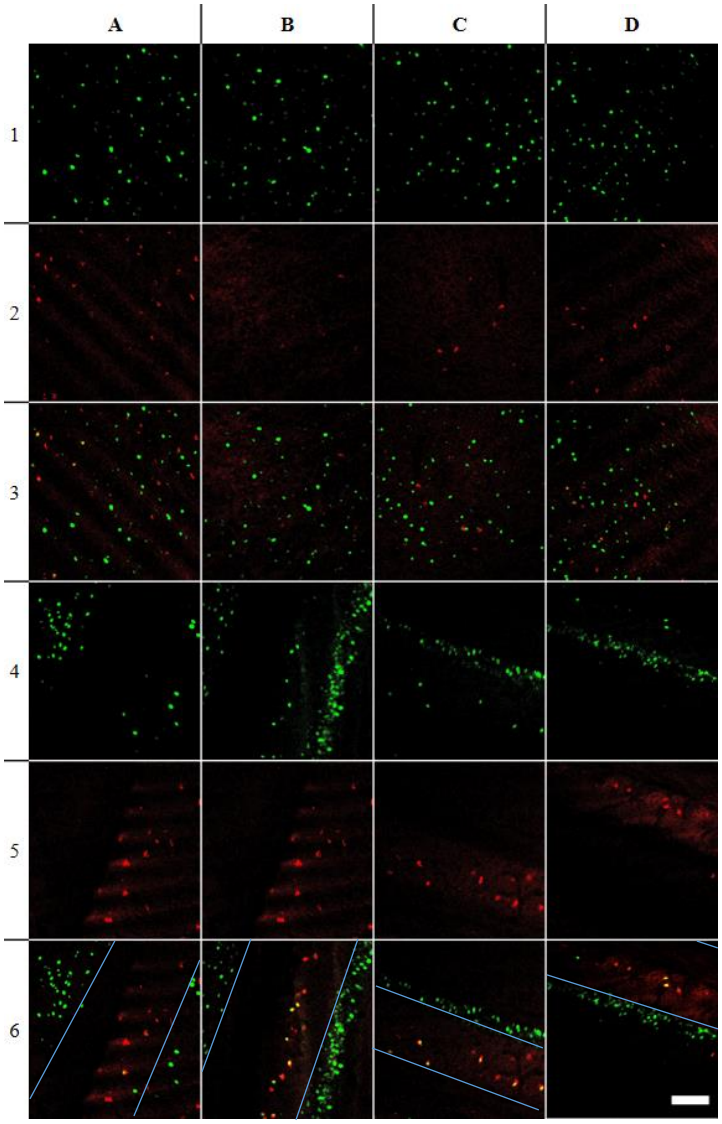

Figure 2: Representative Images of Fos and SST Staining. Columns A-D are male $\gamma2^{f/+}$, female $\gamma2^{f/+}$, male SSTCre:$\gamma2^{f/f}$, and female SSTCre $\gamma2^{f/f}$, respectively. Rows 1-3 are from mPFC. Rows 4-6 are from CA1 of hippocampus. Rows 1 and 4 are Fos staining. Rows 2 and 5 are SST staining. Rows 3 and 6 are merged images. The area within the blue bars in row 6 denotes the region within these images that was considered S. oriens. The scale bar in D6 is is 50 μm. Nuclear Fos staining and cytoplasmic SST staining illustrate successful staining for both cell markers.

3.3 Colocalization of SST and Fos in mPFC and vHipp

After all technical replicate images were acquired for each biological replicate, biological replicate groups were compared against genotype and sex. Images were quantified by thresholding the original image so that only pixels with the top 1% of Fos and 3% of SST signal

intensities were counted, and cells were defined as being 50 pixels or larger. For images that would not allow this high of a threshold, pixel size of positive cells was heightened to 100 pixels to account for the larger number of pixels left after thresholding the image. For images that would not allow this low of a threshold, pixel size of positive cells was lowered to 30 pixels to account for the lower number of pixels left after thresholding the image. After thresholding and scanning for positive cells in both channels within an image, thresholded images were stacked to manually check for colocalization. In this experiment, colocalization was defined as either overlapping or directly juxtaposed Fos and SST signals. Single positive and double positive staining cell counts with SEM bars are shown in Figure 3.

No sex or genotype difference in Fos or SST expression was found in any brain region. After combining sexes, no statistically significant effect was identified; the only statistical trend observed was in the increased ratio of SST^{+}, Fos^{+} cells to total SST^{+} cells in S. oriens of SSTCre:$\gamma2^{f/f}$ mice compared to $\gamma2^{f/+}$ controls (Figure 3D).

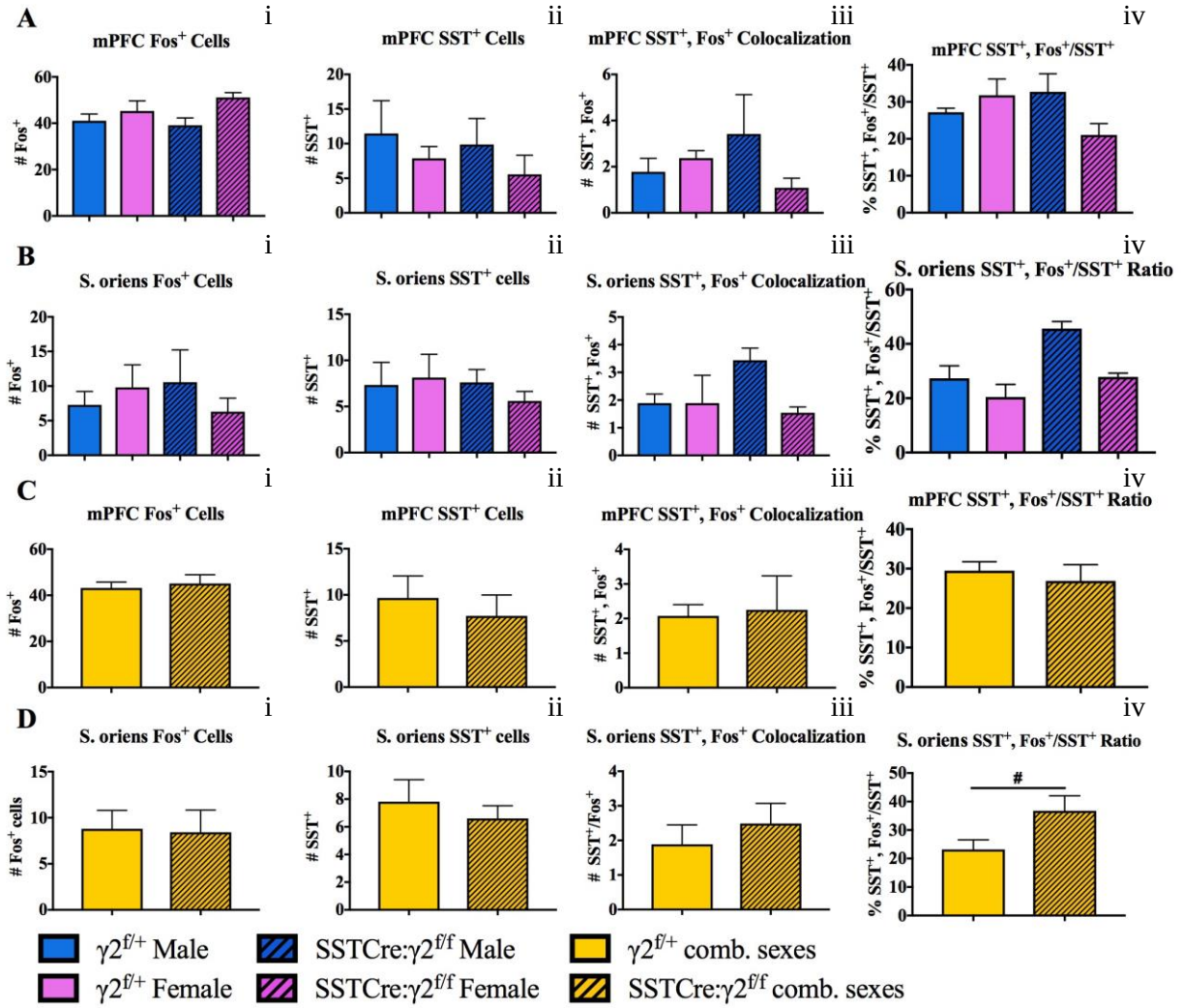

Figure 3: Quantification of the density of Fos$^+$; SST$^+$; SST$^+$, Fos$^+$; and SST$^+$, Fos$^+$/SST$^+$ in the mPFC and S. oriens of vHippocampus of SSTCre:γ2$^{f/f}$ vs. γ2$^{f/+}$ mice. For A and B, subject pools were n=3 for γ2$^{f/+}$ male mPFC, n=3 for γ2$^{f/+}$ female mPFC, n=2 for SSTCre:γ2$^{f/f}$ male mPFC, n=2 for SSTCre:γ2$^{f/f}$ female mPFC, n=2 for γ2$^{f/+}$ male S. oriens, n=3 for γ2$^{f/+}$ female S. oriens, n=2 for SSTCre:γ2$^{f/f}$ male S. oriens, and n=2 for SSTCre:γ2$^{f/f}$ female S. oriens. For C and D, n=5 for γ2$^{f/+}$ mPFC, n=5 for SSTCre:γ2$^{f/f}$ mPFC, n=6 for γ2$^{f/+}$ S. oriens, and n=4 for SSTCre:γ2$^{f/f}$ S. oriens. **(A)** No significant effect in Fos$^+$ (i); SST$^+$ (ii); SST$^+$, Fos$^+$ (iii); or SST$^+$, Fos$^+$/SST$^+$ (iv) in mPFC. **(B)** No significant effect in Fos$^+$ (i); SST$^+$ (ii); SST$^+$, Fos$^+$ (iii); or SST$^+$, Fos$^+$/SST$^+$ (iv) in S. oriens. **(C** No significant effect in Fos$^+$ (i); SST$^+$ (ii); SST$^+$, Fos$^+$ (iii); or SST$^+$, Fos$^+$/SST$^+$ (iv) in mPFC after combining sexes. **(D)** No significant effect in Fos$^+$ (i); SST$^+$ (ii); or SST$^+$, Fos$^+$ (iii). For SST$^+$ Fos$^+$ doubly positive cells normalized to the density of SST$^+$ cells there was a trend of higher Fos$^+$ SST$^+$ cell density in S. oriens in SSTCre:γ2$^{f/f}$ vs. γ2$^{f/+}$ mice (t=2.202, df=7, P=0.0586, two-tailed unpaired t test). See Tables 1 and 2 for summary of statistical tests of all data.

Chapter 4

Discussion

The purpose of this experiment was to elucidate the brain regions implicated in the anxiolytic- and antidepressant-like phenotype found in SSTCre:$\gamma 2^{f/f}$ mice when compared to $\gamma 2^{f/+}$ controls. At the beginning of the study, it was hypothesized that the heightened activity of SST^{+} cells would result in heightened expression of Fos and thus the ratio of SST^{+}, Fos^{+} to all SST^{+} cells would be higher across all brain regions in SSTCre:$\gamma 2^{f/f}$ mice when compared to $\gamma 2^{f/+}$ controls.

The results of my experiment provide moderate evidence that the original hypothesis is true in S. oriens of the CA3 subregion of vHipp and is completely inconclusive for mPFC. The low number of biological replicates for all sex- and genotype-segregated statistical tests limited the interpretability of the results as this made the data non-normal and required the use of a Mann-Whitney test for significance rather than a two-tailed t test. When sexes were combined to check for any genotype effect, the mPFC showed no significant differences in any metric (Table 1). Statistical comparison of sex/genotype groups of S. oriens data did not yield statistically significant genotype effects either (Table 1). Statistical analysis of genotype effect, tests for significance of genotype effect after combining sex groups, were more informative than sex/genotype group comparisons, and no significant trends were found for any staining metric,

with the exception of an increase in SST^+, Fos^+ to total SST^+ ratio in SSTCre:$\gamma2^{f/f}$ S. oriens compared to that of $\gamma2^{f/+}$ controls (Table 2).

mPFC / S.oriens	Male $\gamma2^{f/+}$		Female $\gamma2^{f/+}$		Male SSTCre:$\gamma^{f/f}$		Female SSTCre:$\gamma^{f/f}$	
Male $\gamma2^{f/+}$			Fos^+	0.999	Fos^+	0.800		
			SST^+	0.700	SST^+	0.999		
			+,+	0.400	+,+	0.400		
			+,+/+	0.700	+,+/+	0.400		
Female $\gamma2^{f/+}$	Fos^+	0.800					Fos^+	0.800
	SST^+	0.999					SST^+	0.400
	+,+	0.800					+,+	0.200
	+,+/+	0.400					+,+/+	0.200
Male SSTCre:$\gamma^{f/f}$	Fos^+	0.667					Fos^+	0.333
	SST^+	0.999					SST^+	0.667
	+,+	0.333					+/+	0.333
	+,+/+	0.333					+,+/+	0.333
Female SSTCre:$\gamma^{f/f}$			Fos^+	-0.800	Fos^+	0.667		
			SST^+	0.800	SST^+	0.667		
			+,+	0.800	+,+	0.333		
			+,+/+	0.800	+,+/+	0.333		

Table 1: Statistical Test Information Bank for mPFC and S. oriens Data. The Mann-Whitney U (MW) Test results for each possible genotype/sex/brain region combination is contained in a 2x4 table within a cell of the entire table. The upper right half of the table contains mPFC analysis, and the lower left half of the table is S. oriens analysis. The right column of each cell is the P value of the MW test for that combination and staining metric.

M=male, F=female, γ = $\gamma 2^{f/+}$, S= SSTCre:$\gamma^{f/f}$ Fos^+=Fos positive cell comparison, SST^+=SST positive cell comparison, +,+= SST^+, Fos^+ double positive cell comparison, +,+/+=SST^+, Fos^+ to SST^+, Fos^- cell ratio comparison.

	mPFC, SSTCre:$\gamma^{f/f}$		S. oriens, SSTCre:$\gamma^{f/f}$	
$\gamma 2^{f/+}$	Fos^+	0.668	Fos^+	0.910
	SST^+	0.592	SST^+	0.561
	+,+	0.845	+,+	0.486
	+,+/+	0.566	+,+/+	**0.059**[#]

Table 2: Statistical Test Result Bank for Sex-combined Genotype Comparison Data. The two-tailed unpaired t test results for each possible genotype/brain region is contained in a 2x4 table within a cell of the entire table. The right column of each cell is the P value of the t test for that combination and staining metric. Fos^+=Fos positive cell comparison, SST^+=SST positive cell comparison, +,+= SST^+, Fos^+ double positive cell comparison, +,+/+=SST^+, Fos^+ to SST^+ total cell percentage comparison.

The lack of statistical difference between SST^+ cell counts in both mPFC and S. oriens demonstrates that acute stressors and SSTCre:$\gamma 2^{f/f}$ mutation do not have an effect on the size of SST^+ cell populations in these regions. This data suggests that the hyperactivity of SST^+ cells is not lethal and that their heightened activity and not their disappearance is the cause of anxiolytic- and antidepressant- phenotypes observed in these mice, which was also observed in Western blots in the experiment by Fuchs and Jefferson et al. (2017). Fos expression alone is uninterpretable in my experiment as there is no way to ascertain the relative amount of cells that are expressing Fos, but the lack of statistical difference between genotypes' Fos expression indicates consistency in image capture and absence of bias, a confirmation of blinded quantification.

Interestingly, there was a strong trend of increased ratio of Fos expressing SST^+ cells to all SST^+ in S. oriens but not in mPFC. Ablation of SST^+ interneurons of the frontal cortex has been shown to reduce anxiety-like behavior (Soumier & Sibelle, 2014), which would have supported a high ratio of SST^+, Fos^+ cells in mPFC of SSTCre:$\gamma 2^{f/f}$ mice, but no such effect was found. However, it has also been observed that selective acute activation of excitatory mPFC cells evokes anxiolytic responses (Sthitapranjya et al., 2018), suggesting that the inhibitory transmission of dendrite-targeting SST^+ interneurons may have anxiogenic effects. Moreover, lesions of ventral versus dorsal mPFC elicit distinct activity and biochemical responses in the mPFC-targetted paraventricular nucleus of the hypothalamus (PVH) (Radley et al., 2006), which demonstrates that subregions of the mPFC are heterogeneous in their function and may have different stress-evoked activity. This would mean that measuring Fos expression after an acute stressor in the mPFC as a whole may cause grouping of selectively activated and inactivated subregions and therefore occlude any increase in SST^+, Fos^+ to SST^+ ratio for this brain region. In addition, the designated area (Figure 1B) in which images were taken in mPFC was much larger than that of S. oriens. The lack of genotype effect in my experiment may be caused by a dilution of the effect due to sampling too functionally diverse of a region, which is based on the finding that there are two distinct subpopulations of SST^+ interneurons in mPFC (Kvitsiani et al., 2013), further supporting this rationale.

The trend of SST^+ cells of S. oriens to increase Fos expression following a stressor is indicative of the opposite case of what I just postulated for mPFC: this SST^+ interneuron community represents a specialized and uniform population that experiences heightened excitatory input following stress. A stressor is needed to induce quantifiable amounts of Fos (S Jefferson, personal communication), so any Fos expression found in my experiment can be

assumed to be the result of the forced swim stressor. As such, the increased ratio of SST^+, Fos^+ to all SST^+ cells in S. oriens is directly indicative of this specific interneuron subpopulation being utilized, potentially implicating it as part of the cellular level mechanism anxiolytic- and antidepressant-like behavior. Previous investigation of Fos induction across brain regions have specifically implicated the hippocampus as having the largest increase in *c-fos* mRNA following a 20 minute forced swim stressor (Melia et al., 1994). This increase was also seen in other brain regions such as the cortex, hypothalamus, and brain stem, but the increase in hippocampal *c-fos* mRNA dwarfed all others. In addition, it has been found that reversible inactivation of the ventral hippocampus results in disruption of context-specific fear memory retrieval (Calfa et al., 2007). In terms of neuronal activation and SST^+ cells of vHipp S. oriens, this indicates that the function of this brain region is critical for neural processing of aversive stimuli and is supported by the selective activation of SST^+ cells in this brain region.

The finding that CA1 S. oriens SST^+ interneurons are key in maintenance of acute stress-induced activity but not those of mPFC implicates maintenance of the hippocampal-to-PFC (H-PFC) pathway. The H-PFC pathway is a projection of excitatory glutamatergic neurons from CA1 hippocampus to mainly medial prefrontal cortex, but to lateral and other subregions as well (Barbas & Blatt, 1995). This pathway has also been identified as being particularly vulnerable to stress (McEwen et al., 2007), further corroborating the idea that SST^+ interneurons of CA1 S. oriens are implicated in maintenance of this pathway. In addition, the hippocampal volume of MDD patients has been found to be reduced, reaffirming the idea of hippocampal-mPFC vulnerability to stress (Campbell et al., 2004). Glutamatergic projections from CA1 hippocampus to mPFC are known to innervate glutamatergic principle cells as well as GABAergic interneurons that results in feed-forward inhibition of principle cells activated by these

projections. It then follows that GABAergic interneuron activity of the mPFC would be scaled to glutamatergic cell activity in the hippocampus.

Taken together with anxiety and depression behavior data from Fuchs and Jefferson et al., my data shows that SST^+ interneurons of CA1 experience substantially increased depolarization, and inferentially activity, that results in anxiety- and anhedonia-resistant behavioral phenotypes. This effect is possibly via protection of the stress-vulnerable H-PFC. This would explain why S. oriens SST^+ cells but not those of the mPFC experience increased activity following an acute stressor and suggest that cognitive processing of a stressor by the mPFC is modulated by CA1 network activity.

It is entirely possible, however, that the lack of genotype effect in the mPFC is a product of mPFC being uninvolved in the behavioral phenotype or simply a group size that's too small. To investigate these possibilities and further characterize SST^+ cell activity within the mPFC and CA1 of the ventral hippocampus, group sizes should be enlarged, and a third marker for neuronal nuclei, NeuN, should be added. It goes without saying that increased group size increases the reliability of statistical tests, and the addition of NeuN would allow characterization of the neuronal network around SST^+ cells in terms of how its activity compares to that of SST^+ interneurons. Alternatively, addition of CaMKII antibody would allow analysis of the activity of principle cells in S. pyrimidale and further elucidate the mechanism of network activity maintenance by SST^+ cells. If all three additions were made, the interaction of CA1 pyramidal cells, CA1 SST^+ interneurons, mPFC principle cells, and mPFC SST^+ interneurons could be characterized, and allow insight into the E:I balance maintenance mechanisms behind anxiolytic and antidepressant-like phenotypes in SSTCre:$\gamma 2^{f/f}$ mice.

References

Autry AE, Adachi M, Nosyreva E, Na ES, Los MF, Cheng PF et al. NMDA receptor blockade at rest triggers rapid behavioural antidepressant responses. *Nature.* 2011; **475**: 91–95.

Barbas H, Blatt GJ. Topographically specific hippocampal projections target functionally distinct prefrontal areas in the rhesus monkey. *Hippocampus* 1995; **5**:511-533.

Bremner JD, Innis RB, Southwick SM, Staib L, Zoghbi S, Charney DS. Decreased benzodiazepine receptor binding in prefrontal cortex in combat-related posttraumatic stress disorder. *Am J Psychiatry*. 2000; **157**: 1120–1126.

Buzsaki G, Csicsvari J, Dragoi G, Harris K, Henze D, Hirase H. Homeostatic maintenance of neuronal excitability by burst discharges in vivo. *Cereb Cortex*. 2002; **12**: 893–899.

Calfa G, Bussolino D, Molina VA. Involvement of the lateral septum and the ventral Hippocampus in the emotional sequelae induced by social defeat: role of glucocorticoid receptors. *Behav Brain Res*. 2007;**181**:23–34.

Campbell S, Macqueen G. The role of the hippocampus in the pathophysiology of major depression. *J Psychiatry Neurosci.* 2004; **29**: 417–426.

Cruz FC, K.E., Guez-Barber DH, Bossert JM, Lupica CR, Shaham Y, Hope BT. New technologies for examining the role of neuronal ensembles in drug addiction and fear. *Nat Rev Neurosci.* 2013. **14**(11): 743-754.

Cullinan WE, Herman JP, Watson SJ. Ventral subicular interaction with the hypothalamic paraventricular nucleus: evidence for a relay in the bed nucleus of the stria terminalis. *J Comp Neurol.* 1993; **332**:1–20.

Dragunow M, Faull R. The use of c-fos as a metabolic marker in neuronal pathway tracing. *J Neurosci Meth.* 1989; **29**(3): 261-265.

Earnhart JC, S.C., Crestani F, Iwasato T, Itohara S, Mohler H, et al., GABAergic control of adult hippocampal neurogenesis in relation to behavior indicative of trait anxiety and depression states. *J Neurosci.* 2007; **27**(14): 3845-3854.

Engin E, Stellbrink J, Treit D, Dickson CT. Anxiolytic and antidepressant effects of intracerebroventricularly administered somatostatin: behavioral and neurophysiological evidence. *Neuroscience.* 2008; **157**: 666–676.

Essrich C, Lorez M, Benson JA, Fritschy JM, Lüscher, B. Postsynaptic clustering of major GABAA receptor subtypes requires the gamma 2 subunit and gephyrin. *Nat. Neurosci.* 1998; **1**: 563–571.

Fanselow EE, Richardson KA, Connors BW. Selective, state-dependent activation of somatostatin-expressing inhibitory interneurons in mouse neocortex. *J Neurophysiol*. 2008; **100**: 2640–2652.

Fuchs T, Jefferson SJ, Hopper A, Yee P, Maguire J, Luscher B. Disinhibition of somatostatin positive interneurons results in an anxiolytic and antidepressant-like brain state. *Mol Psychiatry*. 2017; **22**(6): 920-930.

Gilman,M.Z., Wilson.R.N. and Weinberg.R.A. Multiple proteinbinding sites in the 5'-flanking region regulate c-fos expression. *Mol. Cell. Biol*. 1986; **6**: 4305-4316.

Gonchar Y, Wang Q, Burkhalter A. Multiple distinct subtypes of GABAergic neurons in mouse visual cortex identified by triple immunostaining. *Front Neuroanat*. 2007; **1**: 3.

Gunther U, Benson J, Benke D, Fritschy JM, Reyes G, Knoflach F, Crestani F, Aguzzi A, Arigoni M, Lang Y, Bluethmann H, Mohler H, Luscher B. Benzodiazepine-insensitive mice generated by targeted disruption of the gamma 2 subunit gene of gamma-aminobutyric acid type A receptors. *Proc Natl Acad Sci USA*. 1995; **92**: 7749–7753.

Hasler G, v.d.V.J., Tumonis T, Meyers N, Shen J, Drevets WC, Reduced prefrontal glutamate/glutamine and gamma-aminobutyric acid levels in major depression determined using proton magnetic resonance spectroscopy. *Arch Gen Psychiatry*. 2007; **64**(2): 193-200.

Hayes TE, Kitchen AM, Cochran BH. Inducible binding of a factor to the c-fos regulatory region. *Proc Natl Acad Sci*. 1987; **84**:1217-1225.

Klempan TA, Sequeira A, Canetti L, Lalovic A, Ernst C, Ffrench-Mullen J, et al. Altered expression of genes involved in ATP biosynthesis and GABAergic neurotransmission in the ventral prefrontal cortex of suicides with and without major depression. *Mol Psychiatry*. 2009; **14**:175–189.

Kvitsiani D, Ranade S, Hangya B, Taniguchi H, Huang JZ, Kepecs A. Distinct behavioural and network correlates of two interneuron types in prefrontal cortex. *Nature.* 2013; **498**: 363-366.

Leão RN, Mikulovic S, Leão KE, Munguba H, Gezelius H, Enjin A. OLM interneurons differentially modulate CA3 and entorhinal inputs to hippocampal CA1 neurons. *Nat. Neurosci.* 2012; **15**: 1524–1530.

Lin L-C, Sibille E. Reduced brain somatostatin in mood disorders: a common pathophysiological substrate and drug target? *Front Pharmacol*. 2013; **4**:110.

Luscher, B., Shen, Q., and Sahir, N. The GABAergic deficit hypothesis of major depressive disorder. *Mol Psychiatry*. 2011; **16**: 383–406.

Maggio N, Segal M. Differential corticosteroid modulation of inhibitory synaptic currents in the dorsal and ventral hippocampus. *J Neurosci*. 2009; **29**:2857–2866.

Melia KF, Ryabinin AE, Schroeder R, Bloom FE, Wilson MC. Induction and habituation of immediate early gene expression in rat brain by acute and repeated restraint stress. *J Neurosci.* 1994; **14**:5929-5938.

Merali Z, Du L, Hrdina P, Palkovits M, Faludi G, Poulter MO, et al. Dysregulation in the suicide brain: mRNA expression of corticotropin-releasing hormone receptors and GABA(A) receptor subunits in frontal cortical brain region. *J Neurosci*. 2004; **24**:1478–1485.

Niciu MJ, Ionescu DF, Richards EM, Zarate CA., Jr Glutamate and its receptors in the pathophysiology and treatment of major depressive disorder. *J Neural Transm*. 2014; **121**:907–924.

Opal MD, Klenotich SC, Morais M, Bessa J, Winkle J, Doukas D et al. Serotonin 2C receptor antagonists induce fast-onset antidepressant effects. *Mol Psychiatry*. 2014; **19**: 1106–1114.

Pfeffer CK, Xue M, He M, Huang ZJ, Scanziani M. Inhibition of inhibition in visual cortex: the logic of connections between molecularly distinct interneurons. *Nat Neurosci*. 2013;**16**:1068–1076.

Price RB, Shungu DC, Mao X, Nestadt P, Kelly C, Collins KA, et al. Amino acid neurotransmitters assessed by proton magnetic resonance spectroscopy: relationship to treatment resistance in major depressive disorder. *Biol Psychiatry*. 2009; **65**:792–800.

Radley JJ, Arias CM, Sawchenko PE. Regional differentiation of the medial prefrontal cortex in regulating adaptive responses to acute emotional stress. *J Neurosci.* 2006; **26**: 12967–12976.

Ren Z., Pribiag H., Jefferson J.J., Shorey M., Fuchs T., Stellwagen D., et al. (2016): Bidirectional homeostatic regulation of a depression-related brain state by GABAergic deficits and ketamine treatment. *Biol Psychiatry*. 2016; **80**(6): 457-468.

Reynolds GP, Abdul-Monim Z, Neill JC, Zhang ZJ. Calcium binding protein markers of GABA deficits in schizophrenia—postmortem studies and animal models. *Neurotox. Res.* 2004; **6**:57–61.

Sanacora G, Fenton LR, Fasula MK, Rothman DL, Levin Y, Krystal JH, Mason GF. Cortical gamma-aminobutyric acid concentrations in depressed patients receiving cognitive behavioral therapy. *Biol Psychiatry*. 2006; **59**(3): 284-6.

Sanacora G, Gueorguieva R, Epperson CN, Wu YT, Appel M, Rothman DL, Krystal JH, Mason GF. Subtype-specific alterations of gamma-aminobutyric acid and glutamate in patients with major depression. *Arch Gen Psychiatry*. 2004; **61**(7): 705-13.

Sanacora G, Mason GF, Rothman DL, Behar KL, Hyder F, Petroff OA, Berman RM, Charney DS, Krystal JH. Reduced cortical gamma-aminobutyric acid levels in depressed patients determined by proton magnetic resonance spectroscopy. *Arch Gen Psychiatry*. 1999; **56**(11): 1043-7.

Schweizer C, Balsiger S, Bluethmann H, Mansuy M, Fritschy JM, Mohler H, Luscher B. The γ2 subunit of $GABA_A$ receptors is required for maintenance of receptorsat mature synapses. *Mol Cell Neurosci*. 2003; **24**:442–450.

Sequeira A, Mamdani F, Ernst C, Vawter MP, Bunney WE, Lebel V, et al. Global brain gene expression analysis links glutamatergic and GABAergic alterations to suicide and major depression. *PLoS ONE*. 2009; **4**:e6585.

Sheng M, McFadden G, Greenberg ME. Membrane depolarization and calcium induce c-fos transcription via phosphorylation of transcription factor CREB. *Neuron.* 1990; **4**: 571–582.

Smith K., Rudolph U. Anxiety and depression: Mouse genetics and pharmacological approaches to the role of GABAA receptor subtypes. *Neuropharmacology*. 2012; **62**(1): 54-62.

Soumier A, Sibille E. Opposing effects of acute versus chronic blockade of frontal cortex somatostatin-positive inhibitory neurons on behavioral emotionality in mice. *Neuropsychopharmacology.* 2014; **39**: 2252–2262.

Sthitapranjya P, Sood A, Mukhopadhy S, Vaidya VA. Acute pharmacogenetic activation of medial prefrontal cortex excitatory neurons regulates anxiety-like behaviour. *J Biosci.* 2018; **43**:85–95.

Tripp A, Kota RS, Lewis DA, Sibille E. Reduced somatostatin in subgenual anterior cingulate cortex in major depression. *Neurobiol Dis.* 2011; **42**:116–124.

Valjent E, Caboche J, Vanhoutte P. Mitogen-activated protein kinase/extracellular signal-regulated kinase induced gene regulation in brain: a molecular substrate for learning and memory? *Mol Neurobiol* 2001; **23**(2-3): 83-99.

Viau V, Sawchenko PE. Hypophysiotropic neurons of the paraventricular nucleus respond in spatially, temporally, and phenotypically differentiated manners to acute vs. repeated restraint stress: rapid publication. *J Comp Neurol.* 2002; **445**:293–307

Viollet C, Lepousez G, Loudes C, Videau C, Simon A, Epelbaum J, Somatostatinergic systems in brain: Networks and functions. *Mol Cel Endocrinol*. 2008; **286**(1–2): 75-87.

Wang XM, Tresham JJ, Coghlan JP, Scoggins BA. Intracerebroventricular infusion of a cyclic hexapeptide analogue of somatostatin inhibits hemorrhage-induced ACTH release. *Neuroendocrinology*. 1987; **45:** 325–327.

Academic Vita of Christian Morris
christianmorris17@gmail.com

Education

Schreyer Honors College, The Pennsylvania State University – *University Park, PA* 08/2014-05/2018
Bachelor of Science in Molecular and Cell Biology, with Honors in Molecular and Cell Biology

Research Experience

Undergraduate Researcher, *The Luscher Neuroscience Laboratory, Penn State University* 09/2014-05/2018

- Presented posters at Fall 2016 and Spring 2018 ECOS Research Exhibitions
- Technical experience gained: optimization of immunohistochemistry protocol; immunofluorescenct staining; confocal microscopy; genotyping mice via PCR and gel electrophoresis; cardiovascular perfusion of mice; behavioral testing (forced swim test); image quantification using ImageJ

Extracurricular Activities

Participant, *Global Medical Brigades Penn State, Nicaragua March 2015* 03/2015
Study Abroad, *Seville Spring 2016* 01/2016-05/2016
Patient Floor Volunteer, *Mount Nittany Medical Center* 03/2017-05/2018

Awards and Honors

Dean's List 8 Semesters
Paterno Fellows Scholarship 2 Semesters
BMB Summer Undergraduate Research Fund Awardee 2017
Erickson Discovery Grant Awardee 2017